Title
Lgr6 is a stem cell marker in mouse skin squamous cell carcinoma

Journal
Nature Genetics, 49(11)

ISSN
1061-4036

Authors
Huang, Phillips Y
Kandyba, Eve
Jabouille, Arnaud
et al.

Publication Date
2017-11-01

DOI
10.1038/ng.3957

Peer reviewed

HHS Public Access

Author manuscript

Nat Genet. Author manuscript; available in PMC 2018 March 25.

Published in final edited form as:

Nat Genet. 2017 November ; 49(11): 1624–1632. doi:10.1038/ng.3957.

Lgr6 is a stem cell marker in mouse skin squamous carcinomas

Phillips Y. Huang[*,1,2], **Eve Kandyba**[*,1], **Arnaud Jabouille**[1], **Jonas Sjolund**[3], **Atul Kumar**[1], **Kyle Halliwill**[1], **Melissa McCreery**[1], **Reyno DelRosario**[1], **Hio Chung Kang**[4], **Christine E. Wong**[5], **Jost Seibler**[6], **Vincent Beuger**[6], **Maurizio Pellegrino**[7], **Adam Sciambi**[7], **Dennis J. Eastburn**[7], and **Allan Balmain**[1,8]

[1]Helen Diller Family Comprehensive Cancer Center, University of California San Francisco, San Francisco, CA 94158, USA

[2]Genome Institute of Singapore, 60 Biopolis Street, #02-01 Genome Building, Singapore 138672, Singapore

[3]Division of Translational Research, University of Lund, Sweden

[4]Invitae Corp, 1400 16th St, San Francisco, CA 94103

[5]Institute of Cell Biology, ETH, Zurich

[6]Taconic Biosciences GmbH, Neurather Ring 1, 51063 Cologne, Germany

[7]Mission Bio, Inc., 953 Indiana St, San Francisco, CA 94107

[8]Department of Biochemistry and Biophysics, University of California, San Francisco, CA 94158

Abstract

The G-protein-coupled receptors Lgr4/5/6 are *Wnt* signalling mediators, but their functions in squamous carcinomas (SCCs) are unclear. Using lineage tracing in *Lgr5-EGFP-CreERT2*- and *Lgr6-EGFP-CreERT2- Rosa26/Tomato* reporter mice, we demonstrate that *Lgr6*, but not *Lgr5*, acts as an epithelial stem cell marker *in vivo* in SCCs. We identify, by single molecule *in situ* hybridisation and cell sorting, rare Lgr6-positive cells in immortalised keratinocytes, and show that their frequency increases in advanced SCCs. *Lgr6* expression is enriched in cells with stem cell characteristics, and *Lgr6* downregulation *in vivo* causes increased epidermal proliferation, with expanded lineage tracing from $Lgr6^{+}$ epidermal stem cells. Surprisingly, *Lgr6* germline knockout mice are predisposed to SCC development, by a mechanism that includes compensatory upregulation of *Lgr5*. These data provide a model for human patients with germline loss of

Corresponding author abalmain@cc.ucsf.edu; Tel: 415 502 4192; Fax: 415 502 3179 (A.B).
*These authors contributed equally

Author Contributions

P.Y.H., E.K and A.B. designed experiments; Jost Seibler and V.B. generated and provided ES cells for making mouse strains; P.Y.H., E.K, J.S., A.K., R.D., H.C.K., A.J., and C.E.W. performed experiments; P.Y.H., E.K and A.B. analysed data; K.H. and M.McC. carried out statistical analyses, and P.Y.H., E.K and A.B. wrote the manuscript, with contributions from the other authors.

Competing Financial Interests Statement

Dennis Eastburn, Maurizio Pellegrino, and Adam Sciambi are employees of Mission Bio, Inc. Allan Balmain is a member of the Scientific Advisory Board for Mission Bio, Inc.

function mutations in *WNT* pathway genes *RSPO1* or *LGR4*, who show increased susceptibility to squamous tumour development.

Keywords

Lgr6; Lgr5; skin; lineage tracing; stem cells

Introduction

The mouse skin hair follicle (HF) comprises several distinct stem cell populations[1–3]. *Lrig1*[3,4] defines a cell population in the HF junctional zone that serves to maintain the HF infundibulum[5–7], while quiescent *Krt15*-positive stem cells in the bulge region act as a reserve stem cell pool that becomes activated in response to stress[8]. *Lgr4-6* are expressed in stem cells in many tissues, including the small intestine[9], breast[10], ovary[11,12] and haematopoietic system[13]. In the skin, *Lgr5* has been genetically linked to a network of genes that are expressed specifically in the HF[14,15], while *Lgr6* is expressed in the isthmus region, sebaceous gland and interfollicular epidermis[1617].

The Lgr4-6 receptors bind R-spondins (Rspo1-4) to enhance Wnt/β-catenin signalling[18–21]. Wnt signalling is known to be activated in the hair germ and HF bulge during the transition from telogen to anagen phase, and is critical for the formation of new follicles[22–25]. However, several reports have also indicated a negative role for *Lgr5* in Wnt signalling, including in human colorectal cancers[26,27]. Moreover, loss-of-function mutations in human *RSPO1*[28] and *LGR4*[29] increase susceptibility to skin squamous carcinoma development, and *LGR6* has been implicated both as a potential tumour suppressor gene[20], and a breast cancer germline susceptibility gene[30]. Thus, the exact roles of *Lgr4-6* in *Wnt* signalling and tumourigenesis appear to vary depending on the specific *Lgr4-6* and *Rspo1-4* family members that are expressed and interact in a given cellular context[27].

The relationships between normal tissue stem cells and “cancer stem cells” (CSCs, also known as “tumour initiating cells”) are controversial and unresolved[31–35]. Lgr5 has been reported to be a marker of both normal stem cells and CSCs in intestinal adenoma[36], and in gastric cancer[37] but it remains unclear whether members of this gene family are expressed, and in particular play a functional role, in CSCs in other tumour types including cutaneous SCC.

Here, we identify a specific role for *Lgr6* as a cutaneous CSC marker. Expression of *Lgr6*, but not *Lgr5*, increases during tumour progression and metastases, while lineage tracing in established tumours shows that only the progeny of *Lgr6*-positive cells form significant epithelial colonies within SCCs. Nevertheless, germline deletion of *Lgr6* predisposes mice to development of SCCs. These data underline the parallels between this mouse model and human patients with germline loss of genes within this pathway, including *RSPO1* and *LGR4*, who also have increased propensity for SCC development.

Results

Lgr6 is a stem cell marker in squamous carcinoma

Mouse skin SCCs can be initiated with a single dose of Dimethyl-benzanthracene (DMBA) and promoted by repeated treatment with 12-O-tetradecanoyl-phorbol-13-acetate (TPA)[38]. Tumours from this model have common activating mutations in *Ras* oncogenes, and progress through benign and malignant stages, ultimately metastasising to cause the death of the host animals[39]. While the existence of stem cells within tumours in this model has been documented[40], the relationship between these CSCs, and markers of normal stem cells, is unknown. We first analysed published gene expression data from samples of normal skin, papillomas, primary carcinomas and matched metastatic tumours from an interspecific FVBBX backcross population[39]. While *Lgr6* expression continues to rise during progression, *Lgr5* expression shows a decrease, suggesting that Lgr5 may not be required for tumour maintenance (Figure 1a).

We investigated the localised expression of *Lgr5* and *Lgr6* in SCCs from mice carrying an EGFP reporter gene under the control of the *Lgr5* or *Lgr6* promoters (*Lgr5-EGFP-CreERT2* and *Lgr6-EGFP-CreERT2* mice[15,16]). Staining of tumours using antibodies against GFP (Lgr6, green) or Keratin 14 (Krt14, red) (Figure 1b–e and Supp. Fig. 1) showed that *Lgr6* (Fig. 1e), but not *Lgr5* (Fig. 1c), is clearly expressed in distinct colonies of cells distributed through the SCCs. Patterns of co-staining for GFP and Krt14 suggest that while the vast majority of *Lgr6*-positive cells are in the epithelial compartment, the average expression levels of Krt14 in these cells is relatively low compared to the adjacent more differentiated cells (Supp. Fig. 1i, insert). These data are thus compatible with the hypothesis that *Lgr6* may act as a stem cell marker in squamous carcinomas, whereas *Lgr5* does not.

Lgr5^{+} cells have been reported to be capable of acting as the cells-of-origin of intestinal and gastric adenoma[41–43], cutaneous BCC[44] and SCC[45]. Schepers *et al.*[36] exploited the *Lgr5-EGFP-IRES-CreERT2*$^{+/-}$ mouse to activate *Wnt* signalling in the Lgr5-positive crypt stem cells, and showed that the resulting adenomas continued to express *Lgr5*. We asked whether induction of *Ras* mutations within *Lgr5*-positive stem cells in the hair follicle gives rise to SCCs that continue to express *Lgr5*, or if it is dispensable for tumour maintenance. We crossed *Lgr5-EGFP-IRES-CreERT2*$^{+/-}$ or *Lgr6-EGFP-IRES-CreERT2*$^{+/-}$ mice with *Kras*$^{LSL-G12D}$ mice carrying a floxed mutant *Kras* allele[46]. Activation of oncogenic *Kras* with topical 4-hydroxytamoxifen (4OHT) in *Lgr5*-positive stem cells resulted in some limited sebaceous gland hyperplasia (Supp. Fig. 2a), but when the mice were further challenged with a back wound stimulus, papillomas readily arose within 4 weeks (Supp. Fig. 2b). Similar observations were made after activation of *Kras* in the *Lgr6*-positive stem cell population (data not shown). These results are in agreement with the observations of Lapouge *et al.*[47], but contrast with the findings of another study[48] , possibly due to differences in the genetic background of the mice used in different laboratories.

Surgical removal of papillomas in *Lgr5-EGFP-IRES-CreERT2*$^{+/-}$/*Kras*$^{LSL-G12D/+}$ mice led to progression to aggressive spindle carcinomas (Supp. Fig. 2c). *Lgr5* expression could be detected in the outer root sheath (ORS) of HFs in normal skin from *Lgr5-EGFP-IRES-CreERT2*$^{+/-}$/*Kras*$^{LSL-G12D/+}$ mice (Supp. Fig. 2d), or in HFs close to the carcinomas, but not

in the epithelial carcinoma cells (Supp. Fig. 2e). TaqMan and immunofluorescence analyses of 3 independently derived cell lines derived from these spindle carcinomas showed an absence of *Lgr5* expression (Supp. Fig. 2f, g) while *Lgr4* and *Lgr6* expression could readily be detected (Supp. Fig. 2f), We conclude that even tumours arising from *Lgr5*-positive cells in the HF fail to express *Lgr5* during tumour progression, and that *Lgr5* is not a positive driver of SCC growth.

Lineage tracing of *Lgr6*-positive stem cells in squamous tumours

CSCs can give rise to progeny within tumours that continue to fuel tumour development and progression[40,49]. We carried out lineage tracing within chemically induced skin tumours from *Lgr6-EGFP-CreERT2* or *Lgr5-EGFP-CreERT2* mice crossed with *Rosa26-LSL-Tomato* reporter mice[15,16] (hereafter *Lgr6*- or *Lgr5*-reporter mice). Early stage papillomas were induced in both double transgenic lines by standard DMBA treatment followed by 8 weeks of tumour promotion using TPA (Supp. Fig. 3). At this stage, mice were treated with Tamoxifen and papillomas were harvested at different times (2 days, 3 weeks and 6 weeks) thereafter, to measure the extent of lineage tracing from either *Lgr5*- (Fig. 2a, c, e, g) or *Lgr6*-positive (Fig. 2b, d, f, g) stem cells. Imaging of fluorescent cell populations from papillomas 2 days after Tamoxifen treatment identified rare GFP/RFP positive cells in the epithelial compartment in *Lgr6*-reporter mice, but not in Lgr5-reporter mice. (Fig. 2a, b). The number of Tomato-positive traced cells increased at 3 weeks and 6 weeks, giving rise to distinct clones that showed evidence of migration from the initial Lgr6-positive cells (Fig 2d,f). Some Tomato-positive traced cells in *Lgr6*-reporter mice were also observed in the dermis/stromal compartment (Supp. Fig. 4b, d), but these were only a minor population, the significance of which is unknown. In contrast, papillomas from *Lgr5*-reporter mice displayed very few Tomato-positive traced cells, even after 6 weeks, and the majority of these were found in the dermal compartment (Fig. 2e, g and Supp. Fig. 4a, c).

We also carried out lineage tracing from *Lgr6*-positive cells in primary carcinomas that arose between 24–30 weeks after tumour initiation. At 2 days (Fig. 3a,b), 2 weeks (Fig. 3c, d), and 4 weeks (Fig. 3e, f) after tamoxifen treatment there was a significant increase in RFP-positive cell numbers in comparison to papillomas. *Lgr6*-traced RFP-positive clones grew rapidly and occupied a significant proportion of the carcinoma 4 weeks after *Cre* activation (Fig. 4e,f). Again, no significant level of traced progeny cells was seen in the equivalent study of *Lgr5*-reporter mice (Supp. Fig. 5a–d). Interestingly, Driessens *et al*[40] demonstrated that clonal populations arising in skin tumours from *Krt14-CreER/RosaYFP* mice treated with Tamoxifen showed a strong decrease in clone numbers over several weeks, but no such decrease was seen in clone number in our studies of serial biopsies of carcinomas from *Lgr6-CreER/RosaRFP* mice (Fig. 3). This suggests that Krt14 initially labels many transit amplifying cells with poor self-renewal capacity, whereas the Lgr6-positive population is already enriched in stem cells that are capable of long term self renewal.

The transcription factor *Sox2* is expressed in papillomas and squamous carcinomas, and was reported to mark a stem cell population that is enriched in tumour-initiating cells[50]. We investigated possible overlap between Sox2-positive cells and Lgr6-positive cells in SCCs from the DMBA/TPA model by staining for Sox2 in tumours from *Lgr6-EGFP-CreERT2*

mice. The data in Supp. Fig 6 show that *Sox2* is more widely expressed in a larger population of cells than is *Lgr6*, with minimal overlap between the cells expressing these two distinct markers.

Single cell analysis of *Lgr5* and *Lgr6* co-expression in normal keratinocytes and tumour cell lines

Analysis of gene expression at the single cell level is important in the context of CSCs, only a small and variable number of which may be present in solid tumours or tumour cell lines. We carried out gene expression microarray analysis of *Lgr4, 5* and *6* levels in mouse cell lines representing various stages of chemically induced tumours[51,52]. *Lgr5* was not expressed above background levels in any of these cell lines, while *Lgr4* and *Lgr6* were expressed at varying levels (Supp. Fig. 7). Taqman analysis (Fig. 4a), confirmed that *Lgr5* was not expressed above the limits of detection except in positive control back skin samples.

To address the possibility that *Lgr5* may be expressed in rare single cells in keratinocyte cultures, we performed *Lgr4-6* multiplex *in situ* hybridisation[53]. We also analysed a BCC cell line (Asz001)[54], since *Lgr5* has been reported to be expressed in BCC cells. Expression of *Lgr5* was detected in the BCC cells by Taqman and qPCR analyses, albeit at very low levels (Fig. 4b arrow). *In situ* hybridisation analysis revealed that while *Lgr4* was broadly expressed in Asz001 cells, *Lgr5* and *Lgr6* were more restricted in expression. Interestingly, all three family members were co-expressed in rare single cells (Fig. 4c and insets) at a frequency of about 0.75% (4 in 533 cells). This observation raises the intriguing possibility that these rare *Lgr5*, 6 and 4 triple-positive cells are CSCs in the BCC cell line, although further work would be needed to test this hypothesis.

In contrast to the BCC cell line, none of the SCC and keratinocyte cell lines showed significant *Lgr5* expression (Fig. 4d, e, and Supp. Fig. 8). The SCC and keratinocyte cell lines showed different patterns of *Lgr6* expression depending on degree of malignant transformation. In immortalised keratinocytes (C5N, Fig. 4d) and NK cells (Supp. Fig. 8), *Lgr6* was expressed in single cells, together with *Lgr4*. A much larger population of cells expressed *Lgr4* but not *Lgr6*, as also seen in all of the other cell lines tested (Fig. 4 and Supp. Fig. 8). Cell lines derived from tumours at more advanced stages (Fig. 4e: E4 cells, derived from a squamous lung metastasis) showed a high proportion of *Lgr6*-positive cells, in agreement with the observation of high expression levels in these cells by microarray analysis (Supp. Fig. 7). These data therefore demonstrate that, at the single cell level, there appears to be a hierarchy in expression patterns of the *Lgr* gene family. BCCs have distinct *Lgr5*-positive cells, some of which are triple-positive cells that express all three family members. Immortalised keratinocytes lack *Lgr5*, but have rare double-positive *Lgr6* and *Lgr4* cells, and these appear to increase in number in more advanced tumours.

Multiplex analysis of *Lgr* family gene expression using PCR-activated cell sorting (PACS)

To determine the levels of co-expression of *Lgr4-6* at a more quantitative level, we used a novel PCR-activated Cell Sorting (PACS) technology[55–57], (see Materials and Methods). With this method, we were able to identify and sort single cells by performing single-cell TaqMan RT-PCR reactions in >100,000 cells targeting *Lgr4, 5* and *6* mRNA sequences. We

validated this approach using a subset of the cell lines that were analysed for *Lgr* gene expression by *in situ* hybridisation and microarrays. Figure 4f shows that almost 100% of the single NK (immortalised keratinocytes), E4 (metastatic squamous carcinoma cells), and ASZ001 (BCC) cells expressed *Lgr4*, in agreement with the results of *in situ* hybridisation. In contrast, about 1% of the BCC cells expressed *Lgr5*, however, there was no significant expression in NK cells (Fig. 4f). Interestingly, this extremely sensitive approach also identified a small population of E4 cells (around 0.4%) that expressed some *Lgr5* (Fig. 4f) despite the fact that expression analysis by TaqMan (Fig. 4a), microarrays (Supp. Fig. 7), or *in situ* hybridisation (Fig. 4e) of the whole cell population did not detect any significant *Lgr5* transcripts. *Lgr6* was expressed in over 90% of the E4 cells, and in about 10% of BCC cells, but only in about 1–2% of the NK cells, again in line with the *in situ* data (Supp. Fig. 8). We also analysed expression of the same genes in keratinocytes from normal mouse skin. *Lgr4* was quite widely expressed (20–30% of keratinocytes), in agreement with previous data on expression in mouse and human skin [16,58], while *Lgr6*, known to be expressed in the upper isthmus as well as the interfollicular epidermis[16], was found in around 18% and *Lgr5* in around 2% of single keratinocytes (Fig. 4f).

Further analysis of these data (Fig. 4g) confirmed the presence of *Lgr4, 5* and *6* triple positive cells *in vivo* in normal keratinocytes. Around 1.5–2% of normal dorsal telogen skin keratinocytes expressed *Lgr5* (Fig. 4f), and of these about 20% (0.3% of the total population) were triple positive (Fig. 4g). Comparable results were seen for the BCC cell line, where of the 1% of the total cell population that expressed *Lgr5* (Fig. 4f) about 18% (0.18% of the total) were triple positive for all three genes (Fig. 4g). The concordance between *in situ* hybridisation and PACS sorting data for the cell lines indicates that *in vivo* there are specific subpopulations of *Lgr5*-expressing cells that also co-express the other family members. Whether these co-expression patterns are involved in cell fate decisions in normal skin homeostasis *in vivo* remains to be addressed. Interestingly, PACS analysis of primary squamous carcinoma also revealed the presence of a small population of triple positive cells (Supp. Fig. 8d, e). These cells however do not appear to be clonogenic in tumours, as the lineage tracing studies using the *Lgr5-EGFP-CreERT2* allele failed to identify a significant population of traced epithelial tumour cells.

Lgr6 is enriched in keratinocyte cells with stem cell properties

To test the possibility that Lgr6-positive cells represent a stem cell subpopulation, we utilised the Aldefluor assay[59–62] to isolate Aldefluor$^+$ and Aldefluor$^-$ subpopulations from C5N and D3 cultures. *Lgr6* expression was elevated in the Aldefluor$^+$ fraction compared to the Aldefluor$^-$ fraction (Fig. 5a, b), and Aldefluor$^+$ cells sorted from C5N cultures were capable of forming more and larger colonies *in vitro* than Aldefluor$^-$ cells (Fig. 5c). We conclude that Lgr6, and not Lgr5, acts as a marker of a stem-like cell population in squamous epidermal cells.

Lgr6 suppresses epidermal cell growth *in vitro* and *in vivo*

We next overexpressed *Lgr6* in immortalised keratinocytes (NK cells), which have low endogenous levels of *Lgr6* mRNA (Supp. Figs. 7, 8). Transfection of NK cells with an inducible *Lgr6* expression construct (Fig. 5d) led to growth retardation after Doxycycline

treatment (Fig. 5e). To validate this growth suppressive effect of *Lgr6* in epidermal cells, we knocked down *Lgr6* in an SCC cell line (E4), which expresses relatively high endogenous levels of *Lgr6* (Fig. 4e and Supp. Fig. 7). We transduced E4 cells with an inducible *Lgr6* shRNA construct, which, upon doxycycline administration, elicits efficient knockdown of *Lgr6* without altering the levels of either *Lgr4* or *Lgr5* (Fig. 5f). Consistent with a growth suppressive role for *Lgr6* in epidermal cells, doxycycline treatment of transduced E4 cells led to increased growth but had no effect on unmodified E4 cells (Fig. 5g).

Lgr6 knockdown *in vivo* expands lineage tracing in the skin

Lgr6 is a marker of infundibulum stem cells, but a possible functional role in control of homeostasis *in vivo* has not been investigated. Although the *Lgr6*−/− mouse is viable[63], developmental adaptation to loss of expression could lead to compensatory mechanisms for controlling skin homeostasis in the adult mouse. We therefore generated *Lgr6 KD* mice, which possess an *Lgr6* shRNA construct knocked into the *Rosa26* locus that can be induced by doxycycline treatment (Fig. 6a). Adult *Lgr6 KD* mice were treated with doxycycline water for 10 days, leading to an approximately 60% reduction in *Lgr6* expression levels in the back skin, while *Lgr4* and *Lgr5* levels were not significantly affected (Fig. 6b). Immunofluorescence analysis showed that doxycycline administration for this period resulted in an increase in proliferation in the epidermis of *Lgr6 KD* mice, as shown by BrdU labelling (Fig. 6c). These results therefore agree with the *in vitro* data shown in Fig. 5g.

We also tested the effect of *Lgr6* downregulation *in vivo* on patterns of lineage tracing from Lgr6$^+$ stem cells. We generated *Lgr6 KD*$^{+/-}$/*Lgr6-EGFP-IRES-CreERT2*$^{+/-}$/*R26RLacZ*$^{+/-}$ triple transgenic mice, and administered doxycycline to 8-week- old triple transgenic animals and controls for 10 days, followed by activation of Cre recombinase by topical 4OHT treatment. Skin samples were collected 7 days thereafter, and X-Gal analysis revealed a striking increase in the number of *LacZ*-positive cells in the epidermis (Fig. 6d,e,f) in doxycycline-treated mice. This expanded epidermal lineage tracing was accompanied by an increase in the clone size (Fig. 6g), suggesting that *Lgr6* downregulation led to increased proliferation within the *Lgr6* progeny compartment in the epidermis, in line with our observations above (Fig. 6c). It is not possible at this stage to determine whether the increase in traced cells in the epidermis is due to migration from the *Lgr6*-positive cells in the isthmus region, or to independent proliferation of *Lgr6*-positive cells that have been identified within the epidermis[17]. Interestingly, we also saw evidence for *Lgr6* lineage tracing within the dermis, which was particularly elevated in the doxycycline-treated animals (Fig. 6d, lower panel) and has not been previously reported. Control skin from non-4OHT treated adult *Lgr6-EGFP-IRES-CreERT2*$^{+/-}$/R26RLacZ$^{+/-}$ mice showed no staining in either the HFs or the IFE, indicating the non- leakiness of the *Lgr6-EGFP-IRES-CreERT2*$^{+/-}$ promoter construct (Supp. Fig. 9).

Lgr6 activates *Wnt* signalling but is a germline tumour suppressor gene

Lgr5 has been reported to be overexpressed in hepatocellular[64], colon and ovarian cancers[65], and has also been demonstrated to promote the tumourigenicity of BCC cells[66]. Paradoxically, however, *Lgr5* has also been shown to reduce the growth of colorectal cancer cells[26,27], and tumour suppressive roles have been suggested for *Lgr4*[29] and *Lgr6*[20].

Germline loss of *RSPO1*, the upstream ligand for the *Lgr* family of receptors, or of *LGR4*, also causes predisposition to squamous carcinoma development in human patients[28,29]. We therefore investigated the potential role of *Lgr6* as an inducer of *Wnt* signalling in squamous cells, and as a germline tumour suppressor gene.

We assessed the effects of *Lgr6* deregulation on *Wnt* signalling in keratinocyte cell lines using the well characterised TOPFlash assay[67]. Overexpression of *Lgr6* in multiple epidermal cell lines consistently led to activation of this pathway (Fig. 6h). Finally, analysis of human TCGA gene expression data on head and neck SCCs (Supplementary Tables 1 and 2) showed a strong connection to the WNT pathway only for *LGR6*, and not to any significant extent with *LGR5* or *LGR4*. This supports the notion that *LGR6* is linked to *Wnt* signalling and may play a unique role in tumours of squamous origin.

To assess the effect of germline inactivation of *Lgr6* on tumour susceptibility, we bred *Lgr6*−/− mice through multiple generations on to a pure FVB/N genetic background, and exposed them to the DMBA/TPA chemical carcinogenesis protocol. The knockout mice showed a highly significant increase in susceptibility to papilloma development (Fig. 6i), as well as a shortened carcinoma-free survival (Fig. 6j). We conclude that *Lgr6*, in spite of its activity as a positive stimulator of *Wnt* signalling, acts as a germline suppressor of SCC development, thus mimicking the functions of human *WNT* activators *RSPO1* and *LGR4* as SCC suppressor genes. One possible explanation for these apparently contradictory results is that germline loss of *Lgr6* could cause a developmental upregulation of other pathway components that may compensate for loss of *Lgr6* activity. Stem cells in normal skin or intestine display considerable plasticity, such that ablation of Lgr5 positive cells can stimulate their regeneration from alternative stem cell populations[68]. To investigate possible mechanisms of compensation, we derived a series of cell lines from *Lgr6*−/− skin SCCs, and analysed expression levels of the other *Lgr* family members. The wild type mouse carcinomas showed variable activation of the *Wnt* pathway, as demonstrated by the differences in levels of Phospho-β-catenin[69]. Of the three carcinomas tested, highest *Wnt* activity is seen in the cell line (168 cells) that also has the highest level of *Lgr6* expression (left panel, Fig. 6k). Variable levels of *Wnt* activity are also seen in the carcinomas from *Lgr6* knockout mice (right panel, Fig. 6k, Supp. Fig. 11), but in 3 of 4 cases with high activity, the level of *Lgr5* expression is strongly upregulated (arrows). This is particularly significant as all of our expression data show that in SCCs from wild type mice, *Lgr5* is switched off even at the single cell level and plays no significant role as an epithelial cancer stem cell marker. These data therefore identify a mechanism by which cancer stem cells in *Lgr6*−/− mice can be regenerated through a feedback mechanism resulting in upregulation of *Lgr5*.

Discussion

Using a combination of gene expression analysis, lineage tracing, single molecule in situ hybridisation, and PACS analysis of single tumour cells we have shown that *Lgr6* satisfies many of the criteria of an SCC stem cell marker. Lineage tracing identified a subpopulation of *Lgr6*+ tumour cells that give rise to progressively growing epithelial clones. *Lgr6* was enriched in aldefluor-positive cells with stem cell properties, and its inhibition resulted in

increased proliferation and lineage tracing in the epidermis. Although *Lgr5* was not significantly associated with squamous tumour development or progression, it was expressed in rare single cells in a BCC cell line[66], some of which were triple positive for all 3 *Lgr* family members. The detection of these triple positive cells *in vivo* in basal keratinocyte cells, as well as in primary carcinomas, suggests that they may have a distinct role in stem cell homeostasis, but this question will require further investigation.

We believe the model that best explains our results is shown in Supp. Fig. 10. In this model, an early stem cell population may express *Lgr5* and *Lgr6* as well as *Lgr4*, with the initial cell fate choice being determined by competitive interactions of these GPCRs with their R-spondin ligands and other potential effector molecules such as *Rnf43*[70] and *Znrf3*[71]. *Lgr5* expression is maintained in some cells that can give rise to BCCs, but lost in cells that commit to the epidermal cell fate. In this stem cell compartment, *Lgr6* functions as a brake towards further epidermal commitment and differentiation, such that loss of *Lgr6* leads to increased epidermal lineage differentiation and proliferation. It is possible that loss of *Lgr6* expression (but continued expression of *Lgr4*) may be linked to commitment to a more differentiated keratinocyte state. Indeed, the highest levels of *Lgr4* expression are seen in cell lines with the most “epithelial” characteristics such as the immortalised keratinocytes C5N and NK, or the differentiated papilloma cell lines MscP1 or Mscp5 (Supp. Fig. 7).

Germline deletion of *Lgr6* in the mouse caused predisposition to SCC development, as also seen in human patients with germline loss of *LGR4*[29] or *RSPO1*[28]. Tumours that arose in *Lgr6*−/− mice in fact showed upregulation of *Lgr5*, particularly in those tumours with the highest levels of *Wnt* signalling. These data highlight the plasticity and complex control of *Wnt/B-catenin* signalling in the skin, where activation of the pathway can maintain hair follicle[72–74] and epidermal[75] stem cell growth, but impairment in hair follicle stem cells stimulates commitment to the epidermal lineage[73,76–78]. Elevated expression of *β-catenin* is negatively associated with normal epidermal proliferation, but its localisation in the nucleus is positively associated with growth of *Hras*-transformed cells[79]. Successful targeting of the *Wnt* pathway for SCC therapy will require resolution of the complex mechanisms that distinguish signalling in these different biological contexts.

Materials and Methods

Mouse treatments, chemical carcinogenesis and lineage tracing in skin

Lgr6 KD mice were generated in a similar fashion to previously reported doxycycline-inducible knockdown mice[80], using the *Lgr6* shRNA sequence GCATGACACTGGAAGACAACT. Recombinant ES cells were injected into blastocysts and chimeric animals were obtained at the UCSF Cancer Center Transgenic and Targeted Mutagenesis Core Facility. Doxycycline water was prepared by dissolving 2 g of doxycycyline (RPI) in 1 l of water containing 50 g of sucrose (Affymetrix). For BrdU studies, mice were injected intraperitoneally with BrdU labelling reagent (Life Technologies) at a concentration of 10 μL/g of body weight and sacrificed 3 hours post-injection. For chemical carcinogenesis experiments, 8- to 12-week-old male and female mice were randomly assigned to control or treatment groups. Initiation was carried out using a single dose of DMBA (25 ug per mouse in acetone) applied to back skin. One week later,

the mice were administered biweekly topical treatments of TPA (200 uL of a 10-4 M solution in acetone) for 20 weeks. The animals were then monitored for papilloma number and progression to carcinoma. Mice were sacrificed when their first carcinoma reached 1–1.5 cm in diameter. For fluorescent Lgr5/6GFP-Tomato lineage tracing experiments, papillomas were established following the chemical carcinogenesis protocol. After 8 weeks of TPA treatment, one topical dose of Tamoxifen (200 ul of 25 mg/ml in 100% ethanol) was administered to shaved back skin and papillomas were then surgically removed 2 days, 3 weeks and 6 weeks after the initial Tamoxifen treatment for analysis. Similar lineage tracing was carried out with mice bearing carcinomas that arose after 24–30 weeks post initiation with DMBA. To preserve Lgr5/6GFP & Tomato reporter expression, prior to embedding, excised tumours were briefly fixed in 4% paraformaldehyde for 2 hours and then placed in 30% sucrose overnight at 4 °C before freezing in OCT for subsequent cryosectioning. For Lgr6 knockdown lineage tracing experiments, 8- to 10-week-old *Lgr6 KD*$^{+/-}$*/Lgr6-EGFP-IRES-CreERT2*$^{+/-}$*/R26RLacZ*$^{+/-}$ mice were administered either doxycycline water or vehicle for 10 days, and then given one topical dose of 4OHT (1 mg in 200 μl of 100% ethanol) (Sigma-Aldrich) on back skin to induce Cre expression. Mice were sacrificed in triplicates 7 days after induction. Animals were housed in standard conditions, fed *ad libitum* and treated in accordance with the rules and protocols stipulated by the UCSF Institutional Animal Care and Use Committee (IACUC). All mouse experiments were approved by the University of California at San Francisco Laboratory Animal Resource Center. Age-matched animals of the required genotypes were randomly assigned to treatment groups (for instance, wounded or unwounded, Supp. Fig. 2; vehicle- or dox-treated, Fig. 6c–g). When assessing experimental outcomes in animal samples (for instance, BrdU staining in Fig. 6c; X-Gal staining in Fig. 6d–g), investigator was blinded through the use of unique animal IDs for the samples that do not indicate treatment conditions.

X-Gal staining

Back skin samples were surgically removed from 4OHT- or vehicle-treated mice and cut into small pieces. These were added to 4% formaldehyde diluted in PBS, and placed on a shaker at room temperature for 10 min. After 3 washes with PBS, the skin samples were incubated in X-Gal staining solution (1 mg/ml X-Gal, 5 mM $K_3Fe(CN)_6$, 5 mM $K_4Fe(CN)_6$, and 2 mM $MgCl_2$ in PBS) at 37 °C in the dark. The next day, the samples were washed with PBS, transferred to 70% ethanol and made into paraffin blocks. 6 μm sections were cut on a microtome and finally counterstained with nuclear fast red (Vector Laboratories).

Multiplex in situ hybridisation

ViewRNA ISH Cell Assay probes for murine *Lgr4-6* were obtained from Panomics and *in situ* hybridisation was performed, according to the manufacturer's protocol, on cells grown in poly-lysine coated, glass-bottom 96-well plates (In Vitro Scientific). Images were acquired on the 6D high throughput microscope in the UCSF Nikon Imaging Center and analysed using the NIS Elements and ImageJ software packages.

Single-cell RT-PCR analysis

Single cell analysis of *Lgr4*, *Lgr5* and *Lgr6* expression was performed using the Mission Bio, Inc. PACS platform[55–57]. Briefly, single keratinocyte suspensions of disaggregated back

skin, NK cells, E4 SCC cells, BCC cells or primary squamous carcinoma cells were stained with a calcein violet viability dye and encapsulated into microfluidic droplets. Droplets containing individually lysed cells were further processed with the PACS microfluidic workflow to enable droplet-based TaqMan RT-PCR detection of target transcripts. The multiplex RT-PCR reactions consisted of FAM labeled *Lgr5*, HEX labeled *Lgr6* and Cy5 labelled *Lgr4* TaqMan probes. Thermocycling conditions were as follows: 15 min 50 °C, 93 °C for 2 min, 35–40 cycles of 92 °C for 15 s and 60 °C for 1 min. Following thermocycling, the droplets were reinjected into a microfluidic device for fluorescence analysis using four coincident lasers (405 nm, 473 nm, 532 nm, and 640 nm, CNI lasers) to excite the cell viability stain and TaqMan probes. The resulting fluorescence channels (centered at 440 nm, 510 nm, 572 nm, and 680 nm) were separated from the lasers and each other with dichroic filters (Semrock) before being detected by four PMTs (Thorlabs). The detection was processed in real time using LabVIEW and the droplet scatter plots were generated using MATLAB.

Single-cells were analysed with the multiplexed TaqMan assay (7,334 back skin cells, 14,454 NK cells, 21,596 E4 SCC cells, 16,914 BCC cells and 2,617 primary SCC cells). Three independent replicates were performed for each cell/sample type.

Immunofluorescence

First, deparaffinisation and antigen retrieval were performed on 6 μm back skin sections using the Trilogy pretreatment solution (Cell Marque). Then, the sections were incubated in 10% donkey serum (Abcam) diluted in PBS containing 0.3% Triton X-100, at room temperature for 1 hour. Subsequently, the sections were incubated with primary antibody against BrdU (rat, Abcam) or GFP (rabbit, Santa Cruz) at 4 °C overnight. After washing 3 times with PBS containing 0.1% Tween-20, the sections were incubated with the appropriate Alexa 488/555 conjugated secondary antibody (Molecular Probes) for 1 h at room temperature. After washing 3 times with PBS containing 0.1% Tween-20, the samples were finally mounted in Vectorshield hardset mounting medium with DAPI (Vector Laboratories). Lgr5/6GFP and Krt14 expression in primary SCC cryosections was visualised by incubation with anti-GFP (chicken, Abcam) and anti-Krt14 (rabbit, Covance) antibodies, respectively.

Western blot and RT-qPCR analysis

Lgr6 WT and *Lgr6* KO cell lines were derived from SCC generated by DMBA/TPA treatment of WT FVB mice or FVB *Lgr6* −/− mice[67]. SCC were harvested and digested in 4mg ml-1 Collagenase A (Sigma Aldrich) at 37°C for 60 min with agitation, followed by 30 min incubation in 0.25% trypsin-EDTA solution. Dissociated cells were then passed through a 40 μm filter (Greiner Bio-One) and seeded into a 10 cm dish with regular DMEM. For western blot analysis, cells were prepared with lysis buffer (CST) supplemented with protease inhibitors, 100 μM NAF and 100 μM Na_3VO_4. Protein lysates were run by SDS-PAGE and transferred onto PVDF membranes (Biorad). After blocking, membranes were incubated overnight at 4°C with anti phospho β-catenin (#8814; CST) or anti β-actin (#4967; CST) antibodies. Anti Rabbit HRP-linked was used as secondary antibody (#7074; CST). Enhanced Chemoluminescence was used for detection. Phospho β-catenin membrane was stripped for 30 min at room temperature in Restore Plus Stripping buffer (Thermo

Fisher), re-blocked and incubated with anti β-catenin (#1247-1; Epitomics) antibody. For *Lgr* gene expression analysis, RNA was extracted from *Lgr6* WT and *Lgr6* KO cells with TRIzol reagent (Thermo Fisher) and reverse-transcribed using Quantitect RT kit (Qiagen). qPCR expression analyses were performed with the indicated primer sets (Table S3.) by using Power-Up SYBR green mastermix (Thermo Scientific, #A25742) and run on an AB7900HT instrument (Applied Biosystems). Relative gene expression was calculated by using L19 as housekeeping genes to generate ΔCt. ΔCt values from 1425-L1 *Lgr6* WT cells were used as reference to generate ΔΔCt, and relative gene expression was calculated as $2^{(-\Delta\Delta Ct)}$, or presented as copy number/1,000 copies of L19 to calculate gene expression. All reactions were run in duplicate. For primer sequences, see table S3.

Cell culture treatments, MTT and TOPFlash assays

Doxycycline was administered, where appropriate, at a concentration of 1 μg/mL of culture medium. The shRNA sequence used to target *Lgr6* in E4 cells is identical to the one used to generate the *Lgr6 KD* mice (see above) and this was cloned into the doxycycline-inducible F1HtUTG lentiviral vector[81]. For MTT assays, 2000 (*Lgr6* ox and null NK) or 4000 (*Lgr6* shRNA and null E4) cells were seeded in each well of a 96-well plate and the culture medium was replaced every third day. The Vybrant MTT Cell Proliferation Assay (Life Technologies) was performed according to the manufacturer's protocol at the indicated time points after initial seeding. For TOPFlash assays, cells grown in 6-well plates were first transfected with 2 μg of the M50 Super 8x TOPFlash plasmid and 0.1 μg of the pRL-TK renilla luciferase plasmid per well, using Lipofectamine 2000 (Invitrogen). After 6 hours, the medium was replaced and doxycycline was added, where appropriate. 2 days later, luciferase activity was determined for each well using the Dual-Luciferase Reporter Assay System (Promega) with the GloMax Luminometer, according to the manufacturer's instructions.

Cell Lines and Microarray analysis

The cell lines shown in Supplementary Figure 7 were described previously[55,51,82,83] (and references therein). NK cells and C5 cells are immortalised keratinocytes derived from wild type (C5) or Trp53 null mice (NK). Hras null cells were derived from a carcinoma induced by DMBA/TPA in Hras knockout mice[57]. All of the other lines carry initiating mutations in the *Hras* gene. Cells were grown in serum supplemented media into the log phase, then TRIzol RNA extraction was then performed, followed by purification by Qiagen kit. Gene expression analysis of RNA samples from these lines was carried out using Affymetrix M430 2.0 arrays. Microarray CEL files were background corrected and normalised with RMA using oligo in R and then log2 transformed prior to analysis. Cell lines were routinely tested for mycoplasma contamination.

Data Availability

The cell line gene expression microarray data have been deposited in GEO at the time of submission with accession number GSE88742

Aldefluor, colony formation assays and qPCR

Cells cultured *in vitro* were trypsinised and stained with Aldefluor (and DEAB) (Stem Cell Technologies), according to the manufacturer's instructions. The cells were then sorted into Aldefluor^{+} and Aldefluor^{-} fractions on the BD FACSAria III. For expression analyses, RNA was extracted from the sorted cells using TRIzol (Invitrogen), and reverse transcription was performed using the High Capacity Reverse Transcription Kit (Life Technologies). qPCR reactions were subsequently run on the AB7900HT, using Taqman gene expression assays for *Lgr4* (ID Mm00554385_m1), *Lgr5* (ID Mm00438890_m1 and Mm01251804_m1) and *Lgr6* (ID Mm01291336_m1) (Life Technologies). Within each sample, the Ct value for beta-actin was used as a reference to calculate delta Ct values for genes of interest. For each qPCR experiment, all samples were run in technical triplicates and the mean delta Ct value amongst the technical triplicates was determined for genes of interest; all samples were further run in biological triplicates and the data presented show the mean and s.e. amongst these biological triplicates.

For colony formation assays, 2000 cells were seeded in each well of a 6-well plate and grown in a 37 °C cell culture incubator for 19 days. The cells were then fixed in ice-cold methanol for 10 min and finally stained with crystal violet for 10 min.

Statistical analysis

Statistical analyses were carried out using the Prism software package (Graphpad). Significance of difference between two groups was determined using the unpaired, two-tailed Student's t test and labelled as follows: * for $p < 0.05$; ** for $p < 0.01$; and *** for $p < 0.001$. F-tests indicate no evidence of a statistically significant difference in variances of all groups being compared, except in Fig. 5d, 5g (null samples), 6c, 6e and 6h (H11 samples), where Welch's correction is applied. Significance analysis for multiple groups was analysed by ANOVA.

As we could not anticipate an effect size prior to performing our initial experiments, rather than performing a power calculation we defined cohort size by estimating from prior work. We evaluated our prior experimental evidence from unrelated experiments to define a size that allowed us to detect a both statistically as well as practically meaningful difference between the genotypes. In our experiments, using the two-stage carcinogenesis protocol, this is generally between 10 and 20 mice, assuming a less than 5% dropout rate during carcinogenesis.

Supplementary Material

Refer to Web version on PubMed Central for supplementary material.

Acknowledgments

We thank Di Wu, Phuong Thuy Menchavez and Peter Vuong for assistance with handling of mice and RNA samples, and David A. Quigley for help with analysis of microarray data. This work was supported by NCI grants CA084244, CA141455, CA176287 and R01CA184510, and the California Institute for Regenerative Medicine (CIRM) grant TG2-01153 to P.Y.H. Additionally, A.B. acknowledges support from the Barbara Bass Bakar Chair of Cancer Genetics, and P.Y.H. acknowledges support from the Agency for Science, Technology and Research (A*STAR). We are grateful to Fred de Sauvage (Genentech) for provision of the Lgr6−/− mouse strain. The

contents of this publication are solely the responsibility of the authors and do not necessarily represent the official views of CIRM or any other agency of the state of California.

References

1. Blanpain C, Fuchs E. Epidermal homeostasis: a balancing act of stem cells in the skin. Nat Rev Mol Cell Biol. 2009; 10:207–17. [PubMed: 19209183]
2. Jaks V, Kasper M, Toftgard R. The hair follicle-a stem cell zoo. Exp Cell Res. 2010; 316:1422–8. [PubMed: 20338163]
3. Kretzschmar K, Watt FM. Markers of epidermal stem cell subpopulations in adult mammalian skin. Cold Spring Harb Perspect Med. 2014; 4
4. Powell AE, et al. The pan-ErbB negative regulator Lrig1 is an intestinal stem cell marker that functions as a tumor suppressor. Cell. 2012; 149:146–58. [PubMed: 22464327]
5. Jensen KB, et al. Lrig1 expression defines a distinct multipotent stem cell population in mammalian epidermis. Cell Stem Cell. 2009; 4:427–39. [PubMed: 19427292]
6. Page ME, Lombard P, Ng F, Gottgens B, Jensen KB. The epidermis comprises autonomous compartments maintained by distinct stem cell populations. Cell Stem Cell. 2013; 13:471–82. [PubMed: 23954751]
7. Veniaminova NA, et al. Keratin 79 identifies a novel population of migratory epithelial cells that initiates hair canal morphogenesis and regeneration. Development. 2013; 140:4870–80. [PubMed: 24198274]
8. Ito M, et al. Stem cells in the hair follicle bulge contribute to wound repair but not to homeostasis of the epidermis. Nat Med. 2005; 11:1351–4. [PubMed: 16288281]
9. Barker N, et al. Identification of stem cells in small intestine and colon by marker gene Lgr5. Nature. 2007; 449:1003–7. [PubMed: 17934449]
10. Plaks V, et al. Lgr5-expressing cells are sufficient and necessary for postnatal mammary gland organogenesis. Cell Rep. 2013; 3:70–8. [PubMed: 23352663]
11. Flesken-Nikitin A, et al. Ovarian surface epithelium at the junction area contains a cancer-prone stem cell niche. Nature. 2013; 495:241–5. [PubMed: 23467088]
12. Ng A, et al. Lgr5 marks stem/progenitor cells in ovary and tubal epithelia. Nat Cell Biol. 2014; 16:745–57. [PubMed: 24997521]
13. Liu D, et al. Leucine-rich repeat-containing G-protein-coupled Receptor 5 marks short-term hematopoietic stem and progenitor cells during mouse embryonic development. J Biol Chem. 2014; 289:23809–16. [PubMed: 24966324]
14. Quigley DA, et al. Genetic architecture of mouse skin inflammation and tumour susceptibility. Nature. 2009; 458:505–8. [PubMed: 19136944]
15. Jaks V, et al. Lgr5 marks cycling, yet long-lived, hair follicle stem cells. Nat Genet. 2008; 40:1291–9. [PubMed: 18849992]
16. Snippert HJ, et al. Lgr6 marks stem cells in the hair follicle that generate all cell lineages of the skin. Science. 2010; 327:1385–9. [PubMed: 20223988]
17. Fullgrabe A, et al. Dynamics of Lgr6(+) Progenitor Cells in the Hair Follicle, Sebaceous Gland, and Interfollicular Epidermis. Stem Cell Reports. 2015; 5:843–55. [PubMed: 26607954]
18. de Lau W, et al. Lgr5 homologues associate with Wnt receptors and mediate R-spondin signalling. Nature. 2011; 476:293–7. [PubMed: 21727895]
19. Carmon KS, Gong X, Lin Q, Thomas A, Liu Q. R-spondins function as ligands of the orphan receptors LGR4 and LGR5 to regulate Wnt/beta-catenin signaling. Proc Natl Acad Sci U S A. 2011; 108:11452–7. [PubMed: 21693646]
20. Gong X, et al. LGR6 is a high affinity receptor of R-spondins and potentially functions as a tumor suppressor. PLoS One. 2012; 7:e37137. [PubMed: 22615920]
21. Glinka A, et al. LGR4 and LGR5 are R-spondin receptors mediating Wnt/beta-catenin and Wnt/PCP signalling. EMBO Rep. 2011; 12:1055–61. [PubMed: 21909076]

22. Van Mater D, Kolligs FT, Dlugosz AA, Fearon ER. Transient activation of beta -catenin signaling in cutaneous keratinocytes is sufficient to trigger the active growth phase of the hair cycle in mice. Genes Dev. 2003; 17:1219–24. [PubMed: 12756226]
23. Lo Celso C, Prowse DM, Watt FM. Transient activation of beta-catenin signalling in adult mouse epidermis is sufficient to induce new hair follicles but continuous activation is required to maintain hair follicle tumours. Development. 2004; 131:1787–99. [PubMed: 15084463]
24. Lowry WE, et al. Defining the impact of beta-catenin/Tcf transactivation on epithelial stem cells. Genes Dev. 2005; 19:1596–611. [PubMed: 15961525]
25. Greco V, et al. A two-step mechanism for stem cell activation during hair regeneration. Cell Stem Cell. 2009; 4:155–69. [PubMed: 19200804]
26. Walker F, Zhang HH, Odorizzi A, Burgess AW. LGR5 is a negative regulator of tumourigenicity, antagonizes Wnt signalling and regulates cell adhesion in colorectal cancer cell lines. PLoS One. 2011; 6:e22733. [PubMed: 21829496]
27. Wu C, et al. RSPO2-LGR5 signaling has tumour-suppressive activity in colorectal cancer. Nat Commun. 2014; 5:3149. [PubMed: 24476626]
28. Parma P, et al. R-spondin1 is essential in sex determination, skin differentiation and malignancy. Nat Genet. 2006; 38:1304–9. [PubMed: 17041600]
29. Styrkarsdottir U, et al. Nonsense mutation in the LGR4 gene is associated with several human diseases and other traits. Nature. 2013; 497:517–20. [PubMed: 23644456]
30. Garcia-Closas M, et al. Genome-wide association studies identify four ER negative-specific breast cancer risk loci. Nat Genet. 2013; 45:392–8. 398e1–2. [PubMed: 23535733]
31. Perez-Losada J, Balmain A. Stem-cell hierarchy in skin cancer. Nat Rev Cancer. 2003; 3:434–43. [PubMed: 12778133]
32. Visvader JE. Cells of origin in cancer. Nature. 2011; 469:314–22. [PubMed: 21248838]
33. Gonzalez-Suarez E, et al. RANK ligand mediates progestin-induced mammary epithelial proliferation and carcinogenesis. Nature. 2010; 468:103–7. [PubMed: 20881963]
34. Schramek D, et al. Osteoclast differentiation factor RANKL controls development of progestin-driven mammary cancer. Nature. 2010; 468:98–102. [PubMed: 20881962]
35. Gupta PB, Chaffer CL, Weinberg RA. Cancer stem cells: mirage or reality? Nat Med. 2009; 15:1010–2. [PubMed: 19734877]
36. Schepers AG, et al. Lineage tracing reveals Lgr5+ stem cell activity in mouse intestinal adenomas. Science. 2012; 337:730–5. [PubMed: 22855427]
37. Li XB, et al. Gastric Lgr5(+) stem cells are the cellular origin of invasive intestinal-type gastric cancer in mice. Cell Res. 2016; 26:838–49. [PubMed: 27091432]
38. Balmain A, Yuspa SH. Milestones in skin carcinogenesis: the biology of multistage carcinogenesis. J Invest Dermatol. 2014; 134:E2–7. [PubMed: 25302469]
39. McCreery MQ, et al. Evolution of metastasis revealed by mutational landscapes of chemically induced skin cancers. Nat Med. 2015; 21:1514–20. [PubMed: 26523969]
40. Driessens G, Beck B, Caauwe A, Simons BD, Blanpain C. Defining the mode of tumour growth by clonal analysis. Nature. 2012; 488:527–30. [PubMed: 22854777]
41. Barker N, et al. Crypt stem cells as the cells-of-origin of intestinal cancer. Nature. 2009; 457:608–11. [PubMed: 19092804]
42. Barker N, et al. Lgr5(+ve) stem cells drive self-renewal in the stomach and build long-lived gastric units in vitro. Cell Stem Cell. 2010; 6:25–36. [PubMed: 20085740]
43. Zhu L, et al. Prominin 1 marks intestinal stem cells that are susceptible to neoplastic transformation. Nature. 2009; 457:603–7. [PubMed: 19092805]
44. Grachtchouk M, et al. Basal cell carcinomas in mice arise from hair follicle stem cells and multiple epithelial progenitor populations. J Clin Invest. 2011; 121:1768–81. [PubMed: 21519145]
45. da Silva-Diz V, et al. Progeny of Lgr5-expressing hair follicle stem cell contributes to papillomavirus-induced tumor development in epidermis. Oncogene. 2013; 32:3732–43. [PubMed: 22945646]
46. Jackson EL, et al. Analysis of lung tumor initiation and progression using conditional expression of oncogenic K-ras. Genes Dev. 2001; 15:3243–8. [PubMed: 11751630]

47. Lapouge G, et al. Skin squamous cell carcinoma propagating cells increase with tumour progression and invasiveness. EMBO J. 2012; 31:4563–75. [PubMed: 23188079]
48. White AC, et al. Stem cell quiescence acts as a tumour suppressor in squamous tumours. Nat Cell Biol. 2014; 16:99–107. [PubMed: 24335650]
49. Chen J, et al. A restricted cell population propagates glioblastoma growth after chemotherapy. Nature. 2012; 488:522–6. [PubMed: 22854781]
50. Boumahdi S, et al. SOX2 controls tumour initiation and cancer stem-cell functions in squamous-cell carcinoma. Nature. 2014; 511:246–50. [PubMed: 24909994]
51. Oft M, Akhurst RJ, Balmain A. Metastasis is driven by sequential elevation of H-ras and Smad2 levels. Nat Cell Biol. 2002; 4:487–94. [PubMed: 12105419]
52. Wong CE, et al. Inflammation and Hras signaling control epithelial-mesenchymal transition during skin tumor progression. Genes Dev. 2013; 27:670–82. [PubMed: 23512660]
53. Yu M, et al. RNA sequencing of pancreatic circulating tumour cells implicates WNT signalling in metastasis. Nature. 2012; 487:510–3. [PubMed: 22763454]
54. Aszterbaum M, et al. Ultraviolet and ionizing radiation enhance the growth of BCCs and trichoblastomas in patched heterozygous knockout mice. Nat Med. 1999; 5:1285–91. [PubMed: 10545995]
55. Eastburn DJ, Sciambi A, Abate AR. Identification and genetic analysis of cancer cells with PCR-activated cell sorting. Nucleic Acids Res. 2014; 42:e128. [PubMed: 25030902]
56. Eastburn DJ, Sciambi A, Abate AR. Ultrahigh-throughput Mammalian single-cell reverse-transcriptase polymerase chain reaction in microfluidic drops. Anal Chem. 2013; 85:8016–21. [PubMed: 23885761]
57. Pellegrino M, et al. RNA-Seq following PCR-based sorting reveals rare cell transcriptional signatures. BMC Genomics. 2016; 17:361. [PubMed: 27189161]
58. Yi J, et al. Analysis of LGR4 receptor distribution in human and mouse tissues. PLoS One. 2013; 8:e78144. [PubMed: 24205130]
59. Charafe-Jauffret E, et al. Breast cancer cell lines contain functional cancer stem cells with metastatic capacity and a distinct molecular signature. Cancer Res. 2009; 69:1302–13. [PubMed: 19190339]
60. Cheung AM, et al. Aldehyde dehydrogenase activity in leukemic blasts defines a subgroup of acute myeloid leukemia with adverse prognosis and superior NOD/SCID engrafting potential. Leukemia. 2007; 21:1423–30. [PubMed: 17476279]
61. Ginestier C, et al. ALDH1 is a marker of normal and malignant human mammary stem cells and a predictor of poor clinical outcome. Cell Stem Cell. 2007; 1:555–67. [PubMed: 18371393]
62. Corti S, et al. Identification of a primitive brain-derived neural stem cell population based on aldehyde dehydrogenase activity. Stem Cells. 2006; 24:975–85. [PubMed: 16293577]
63. Tang T, et al. A mouse knockout library for secreted and transmembrane proteins. Nat Biotechnol. 2010; 28:749–55. [PubMed: 20562862]
64. Yamamoto Y, et al. Overexpression of orphan G-protein-coupled receptor, Gpr49, in human hepatocellular carcinomas with beta-catenin mutations. Hepatology. 2003; 37:528–33. [PubMed: 12601349]
65. McClanahan T, et al. Identification of overexpression of orphan G protein-coupled receptor GPR49 in human colon and ovarian primary tumors. Cancer Biol Ther. 2006; 5:419–26. [PubMed: 16575208]
66. Tanese K, et al. G-protein-coupled receptor GPR49 is up-regulated in basal cell carcinoma and promotes cell proliferation and tumor formation. Am J Pathol. 2008; 173:835–43. [PubMed: 18688030]
67. Korinek V, et al. Constitutive transcriptional activation by a beta-catenin-Tcf complex in APC−/− colon carcinoma. Science. 1997; 275:1784–7. [PubMed: 9065401]
68. Tian H, et al. A reserve stem cell population in small intestine renders Lgr5-positive cells dispensable. Nature. 2011; 478:255–9. [PubMed: 21927002]
69. Wang MT, et al. K-Ras Promotes Tumorigenicity through Suppression of Non-canonical Wnt Signaling. Cell. 2015; 163:1237–51. [PubMed: 26590425]

70. Koo BK, et al. Tumour suppressor RNF43 is a stem-cell E3 ligase that induces endocytosis of Wnt receptors. Nature. 2012; 488:665–9. [PubMed: 22895187]
71. Hao HX, et al. ZNRF3 promotes Wnt receptor turnover in an R-spondin-sensitive manner. Nature. 2012; 485:195–200. [PubMed: 22575959]
72. Gat U, DasGupta R, Degenstein L, Fuchs E. De Novo hair follicle morphogenesis and hair tumors in mice expressing a truncated beta-catenin in skin. Cell. 1998; 95:605–14. [PubMed: 9845363]
73. Huelsken J, Vogel R, Erdmann B, Cotsarelis G, Birchmeier W. beta-Catenin controls hair follicle morphogenesis and stem cell differentiation in the skin. Cell. 2001; 105:533–45. [PubMed: 11371349]
74. van Genderen C, et al. Development of several organs that require inductive epithelial-mesenchymal interactions is impaired in LEF-1-deficient mice. Genes Dev. 1994; 8:2691–703. [PubMed: 7958926]
75. Lim X, et al. Interfollicular epidermal stem cells self-renew via autocrine Wnt signaling. Science. 2013; 342:1226–30. [PubMed: 24311688]
76. Merrill BJ, Gat U, DasGupta R, Fuchs E. Tcf3 and Lef1 regulate lineage differentiation of multipotent stem cells in skin. Genes Dev. 2001; 15:1688–705. [PubMed: 11445543]
77. Niemann C, Owens DM, Hulsken J, Birchmeier W, Watt FM. Expression of DeltaNLef1 in mouse epidermis results in differentiation of hair follicles into squamous epidermal cysts and formation of skin tumours. Development. 2002; 129:95–109. [PubMed: 11782404]
78. Choi YS, et al. Distinct functions for Wnt/beta-catenin in hair follicle stem cell proliferation and survival and interfollicular epidermal homeostasis. Cell Stem Cell. 2013; 13:720–33. [PubMed: 24315444]
79. Beronja S, et al. RNAi screens in mice identify physiological regulators of oncogenic growth. Nature. 2013; 501:185–90. [PubMed: 23945586]
80. Seibler J, et al. Reversible gene knockdown in mice using a tight, inducible shRNA expression system. Nucleic Acids Res. 2007; 35:e54. [PubMed: 17376804]
81. Herold MJ, van den Brandt J, Seibler J, Reichardt HM. Inducible and reversible gene silencing by stable integration of an shRNA-encoding lentivirus in transgenic rats. Proc Natl Acad Sci U S A. 2008; 105:18507–12. [PubMed: 19017805]
82. Quintanilla M, et al. Comparison of ras activation during epidermal carcinogenesis in vitro and in vivo. Carcinogenesis. 1991; 12:1875–81. [PubMed: 1934268]
83. Portella G, et al. Molecular mechanisms of invasion and metastasis during mouse skin tumour progression. Invasion Metastasis. 1994; 14:7–16. [PubMed: 7657534]

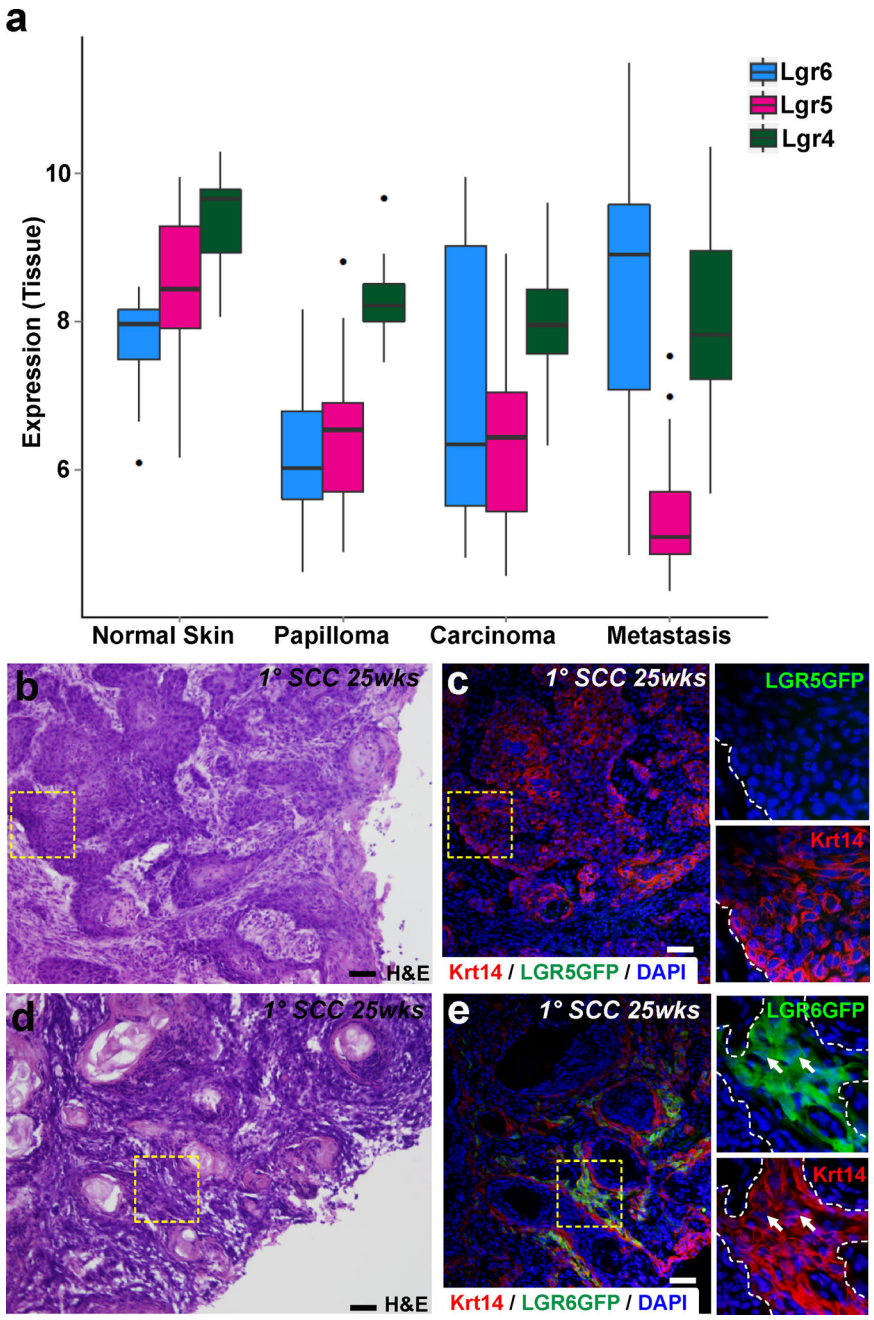

Figure 1. Lgr6 expression increases with squamous tumour progression and Lgr6GFP+ cells, not Lgr5GFP+ cells, are localised within tumour epithelium

Levels of *Lgr5* and *Lgr6* expression during tumour progression were analysed in samples of normal skin, papillomas, primary carcinomas and matched metastatic tumours from an interspecific FVBBX backcross population. (**a**) *Lgr6* expression continues to rise through benign, malignant carcinoma and metastasis stages, while *Lgr5* expression shows a progressive decrease. Localised expression of *Lgr5GFP* and *Lgr6GFP* was investigated within primary squamous carcinomas (at 25wks after initial TPA treatment) by immunostaining against GFP (green) or Keratin 14 (Krt14, red) to identify cell populations specifically expressing stem cell or basal cell markers. (**b−e**) Representative sections from

squamous tumours demonstrating that *Lgr6GFP* (**e**, arrows), but not *Lgr5GFP* (**c**), is clearly expressed in distinct colonies of cells distributed through the SCCs. (**b, d**) H&E staining of serial sections of immunostaining depicted in (**c**) and (**e**), respectively. Yellow dotted boxes demarcate magnified regions of interest in (**c**) and (**e**). White dotted line indicates epithelial border indicated by Krt14 (red) expression. DAPI staining (blue) localises cell nuclei. Scale bar = 50μm.

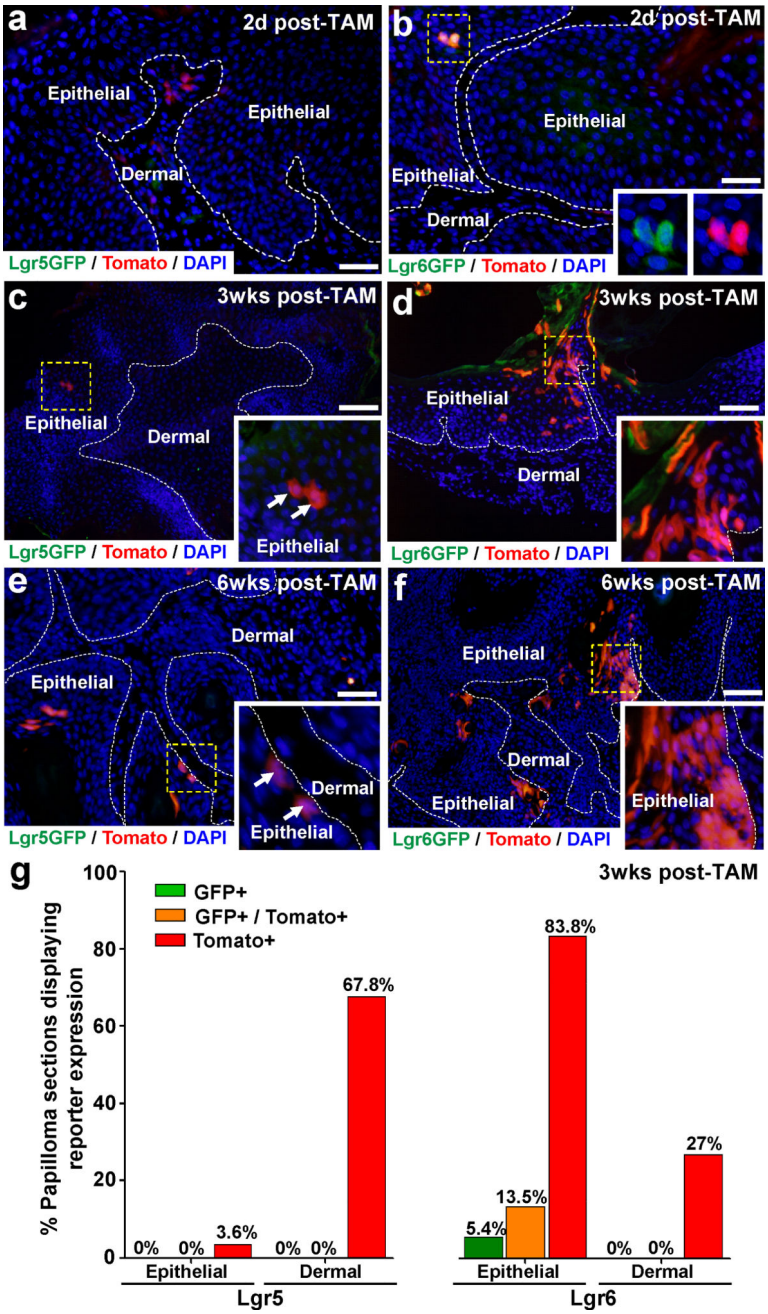

Figure 2. Lgr6-derived clonal expansion is observed in benign squamous tumours

Lgr5- and Lgr6-derived lineage tracing was performed within chemically induced skin tumours from *Lgr6-EGFP-CreERT2* or *Lgr5-EGFP-CreERT2* mice crossed with *Rosa26-LSL-Tomato* reporter mice by standard DMBA treatment followed by 8 weeks of tumour promotion using TPA. Mice were then treated with Tamoxifen (TAM) and papillomas were harvested at 2 days, 3 weeks and 6 weeks thereafter, to measure the extent of lineage tracing from either *Lgr5GFP*- or *Lgr6GFP*-positive stem cells. (**a**) At 2 days post- TAM, no Lgr5-derived Tomato+ cells (red) were readily observed in papilloma epithelium, however, in *Lgr6*-reporter mice, rare Lgr6GFP+Tomato+ cells were localised in the epithelial

compartment (**b**). (**c, e, g**) Over time, rare Lgr5-derived, Tomato+ cells (arrow) were observed in papilloma epithelium, in contrast, Lgr6-derived, Tomato+ traced cell numbers increased at 3 weeks (**g**) and 6 weeks, giving rise to distinct epithelial clones (**d,f**). Yellow dotted box demarcates the magnified regions in the figure insets. White dotted line indicates epithelial-dermal border. DAPI staining (blue) localises cell nuclei. Scale bar = 50μm.

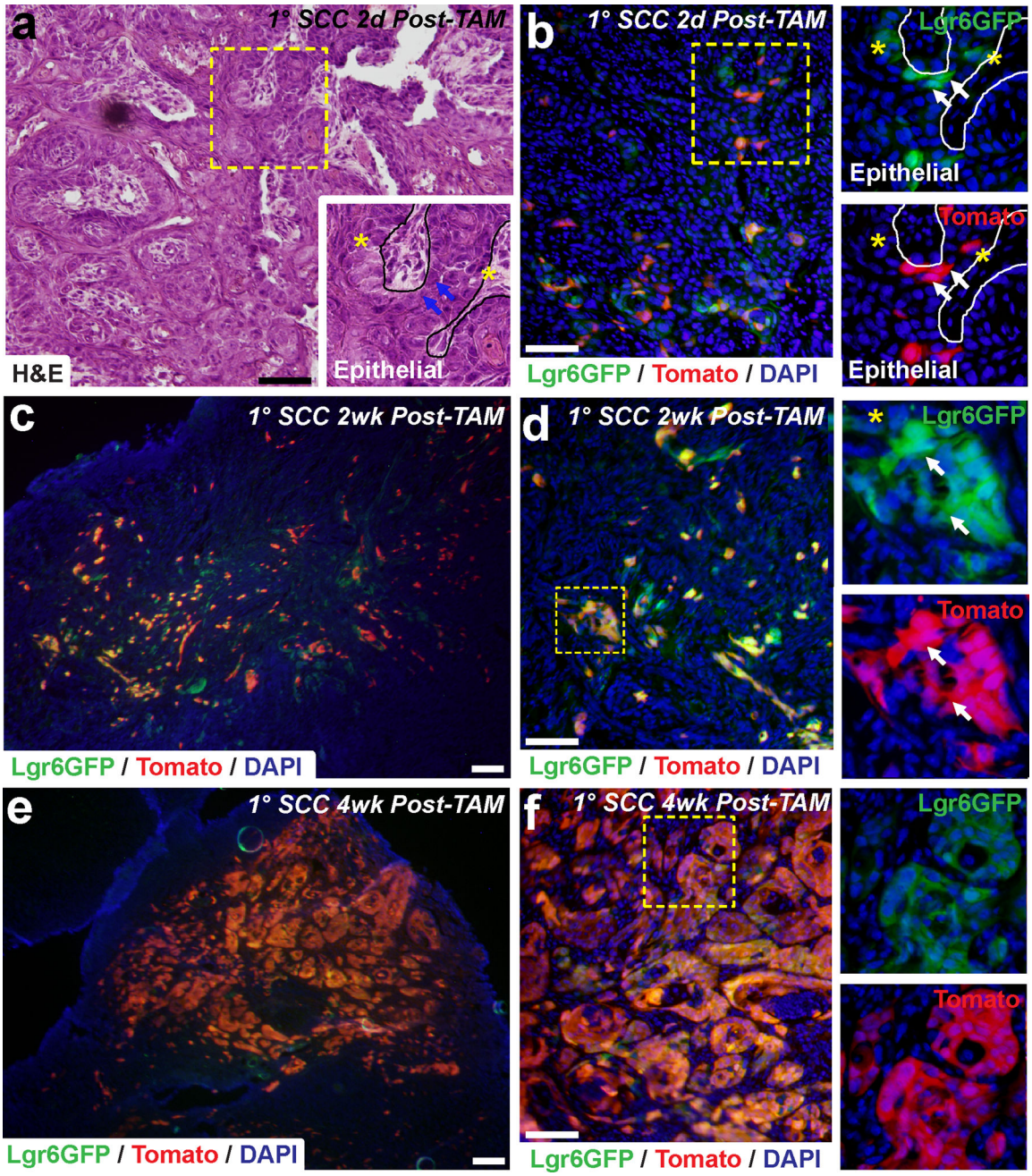

Figure 3. Lgr6-derived clonal expansion in primary SCCs

Lgr6-derived lineage tracing was performed within chemically induced primary (1°) SCCs from *Lgr6-EGFP-CreERT2* mice crossed with *Rosa26-LSL-Tomato* reporter mice by standard DMBA treatment followed by 20 weeks of tumour promotion using TPA. Once SCCs were readily visible, mice were treated with Tamoxifen (TAM) and a biopsy was taken 2 days later, showing abundant *Lgr6GFP*+Tomato+ cells (red) localised in the epithelial compartment (b) as well as some *Lgr6GFP*+ cells (green, *) lacking recombination. (c,d) In the same tumour 2 weeks after TAM treatment, distinct *Lgr6GFP*+/Tomato+ clones were observed (**d**, inset) and at 4wks post-labelling (**e, f**), substantial Tomato+ cell labelling was

observed within the epithelial tumour tissue. Yellow dotted box demarcates the magnified regions in the figure insets. White line indicates epithelial-dermal border. DAPI (blue) staining was used to visualise cell nuclei. (**a**) H&E sections of images depicted in (**b**) to provide tumour histology. Scale bar = 50μm.

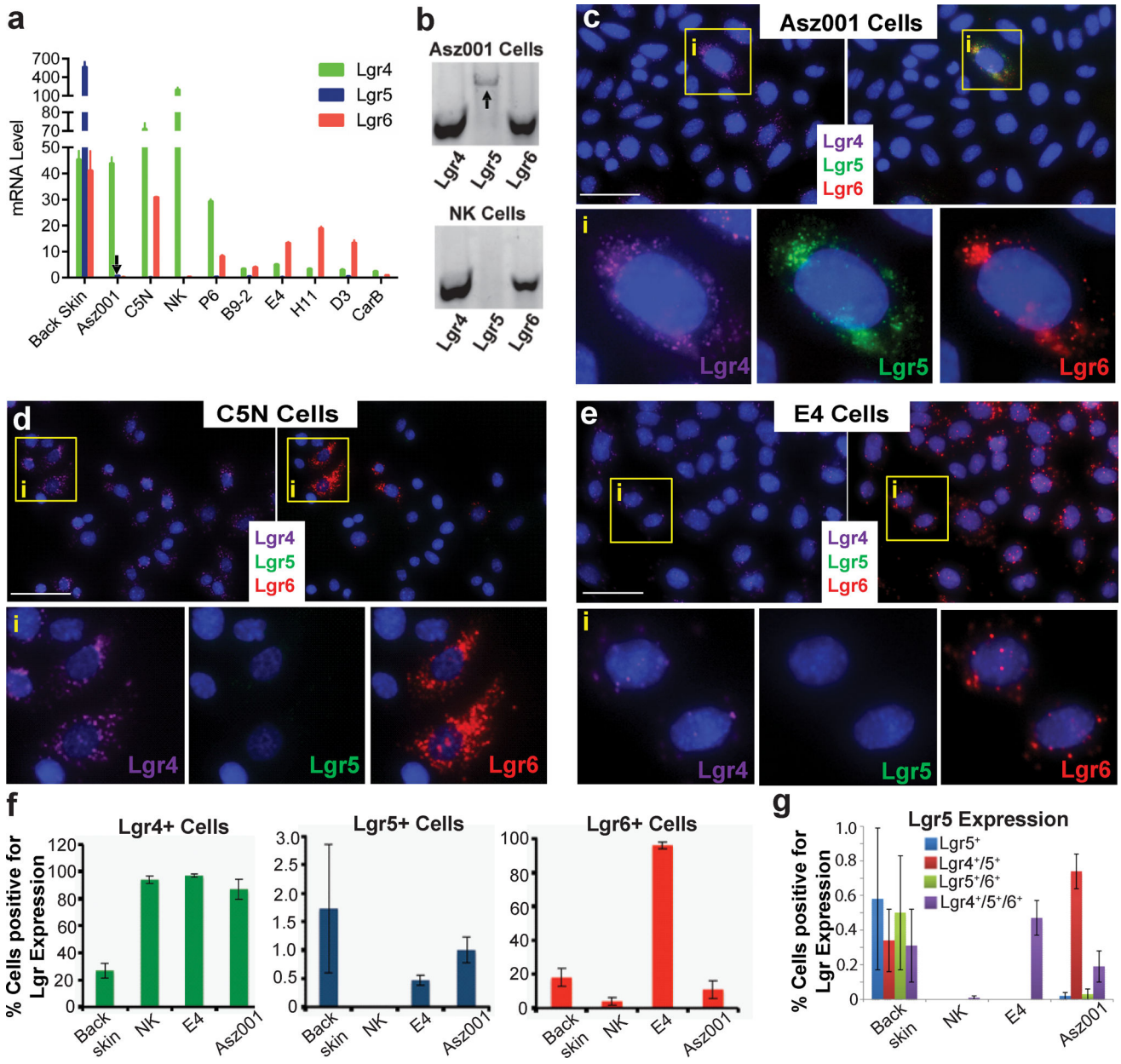

Figure 4. Lgr5 is expressed in rare single BCC cells but not in SCC cells / Lgr6, and not Lgr5, is an SCC CSC marker

(**a**) Taqman analysis showing the expression of *Lgr4-6* in a panel of BCC (Asz001), immortalised keratinocyte (C5N, NK), papilloma (P6), SCC (B9-2, E4) and spindle carcinoma (D3, H11, CarB) cell lines, and control normal back skin samples. Data are presented as mean ± s.e. n = 3. Arrow indicates *Lgr5* expression in Asz001. (**b**) rt-PCR analysis showing the expression of *Lgr4-6* in RNA extracted from a Asz001 sample (above) and a NK sample (below). *Lgr4-6* multiplex *in situ* hybridisation was performed in Asz001 BCC cells. Repeat rt-PCR using biological replicates of Asz001 and NK samples shows the same results. (**c**), immortalised keratinocytes (C5N) (**d**) and E4 SCC cells (**e**). The *Lgr4* (purple) expression pattern is shown in the left panel, while both *Lgr5* (green) and *Lgr6* (red)

expression patterns are shown in the right panels. Yellow asterisks point to cells of interest in each cell line. (**f**) PCR-activated cell sorting (PACS) analysis of *Lgr4-6* expression in dorsal back skin, NK cells, E4 SCC cells and Asz001 BCC cells, n=3. Scale bar = 50 μm.

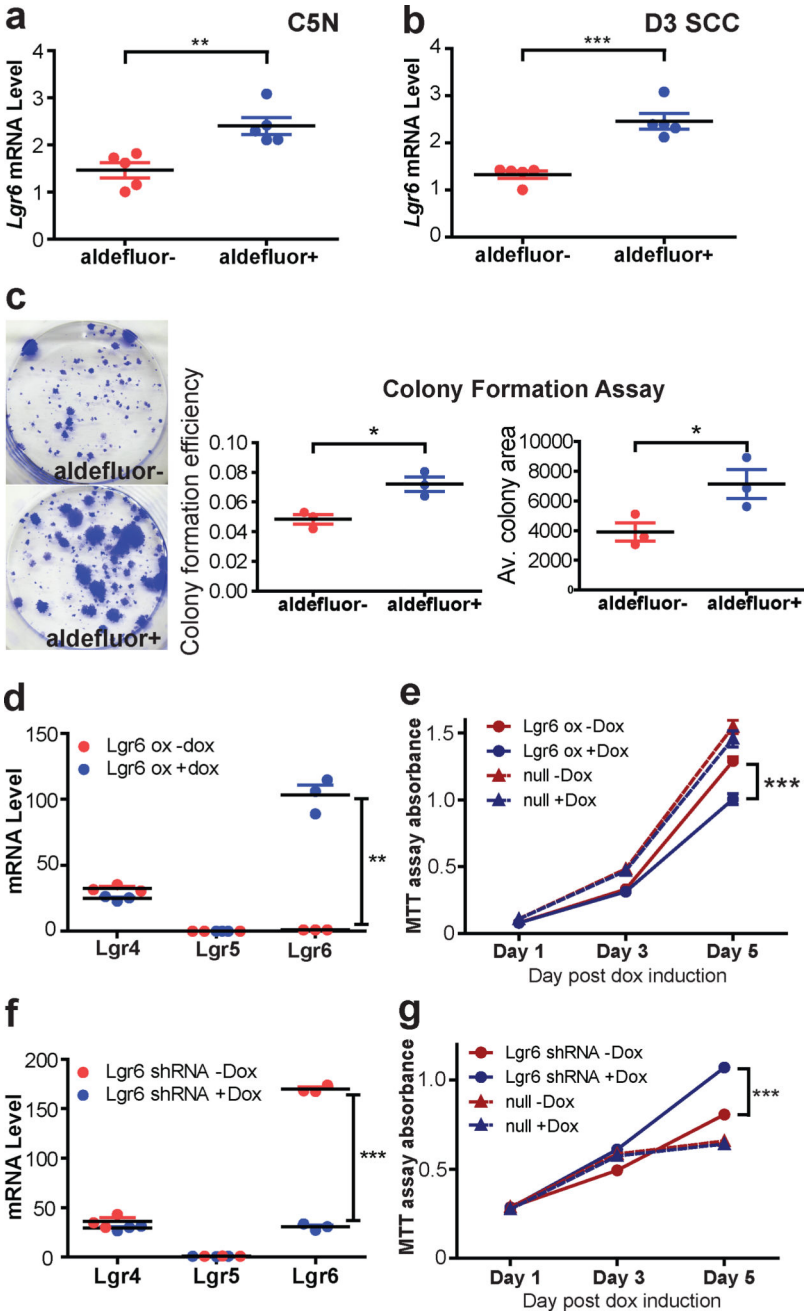

Figure 5. Lgr6 is enriched in epidermal cells with stem cell properties and has growth inhibitory effects in epidermal cell lines

(**a,b**) Putative stem cell subpopulations were isolated from immortalised keratinocytes (C5N) (**a**) and SCC cells (D3) (**b**) based on enrichment for Aldefluor activity. *Lgr6* expression level was determined in the sorted Aldefluor^{+} and Aldefluor^{-} populations using Taqman analysis. (**c**) Normal epidermal cells (C5N) were sorted into Aldefluor^{-} and Aldefluor^{+} subpopulations and these were separately seeded at low density (2000 cells per well) in 6-well plates. Colonies were allowed to grow for 19 days before being visualised by staining with crystal violet. (**c**) Representative wells showing colony formation by

Aldefluor^{-} cells (left) and Aldefluor^{+} cells (right). For each well, the colonies were manually counted and the cell area was calculated in ImageJ to determine the colony formation efficiency and average colony area (**c**). Data are presented as mean ± s.e. *p < 0.05, **p < 0.01 and ***p < 0.001. n = 5 for (**a**) and (**b**), and n = 3 for (**c**). (**d,e**) Immortalised keratinocytes (NK) were transduced with an inducible Lgr6 expression construct (Lgr6 ox cells) or left unmodified (null cells). The cells were then grown either in the presence of absence of doxycycline, and growth was monitored at various timepoints using the MTT assay. (**d**) Taqman analysis showing *Lgr4-6* mRNA levels in Lgr6 ox NK cells after 3 days of growth in the presence or absence of doxycycline. (**e**) Growth curves of Lgr6 ox or null NK cells cultured in the presence or absence of doxycycline. (**f,g**) SCC cells (E4) were transduced with an inducible *Lgr6 shRNA* construct (Lgr6 shRNA cells) or left unmodified (null cells). The cells were then grown either in the presence or absence of doxycycline, and growth was monitored at various timepoints using the MTT assay. (**f**) Taqman analysis showing *Lgr4-6* mRNA levels in Lgr6 shRNA E4 cells after 3 days of growth in the presence or absence of doxycycline. (**g**) Growth curves of Lgr6 shRNA or null E4 cells cultured in the presence or absence of doxycycline. Data are presented as mean ± s.e. ***p < 0.001 and **p < 0.01. n = 3 for (**d**) and (**f**), and n = 5 for (**e**) and (**g**).

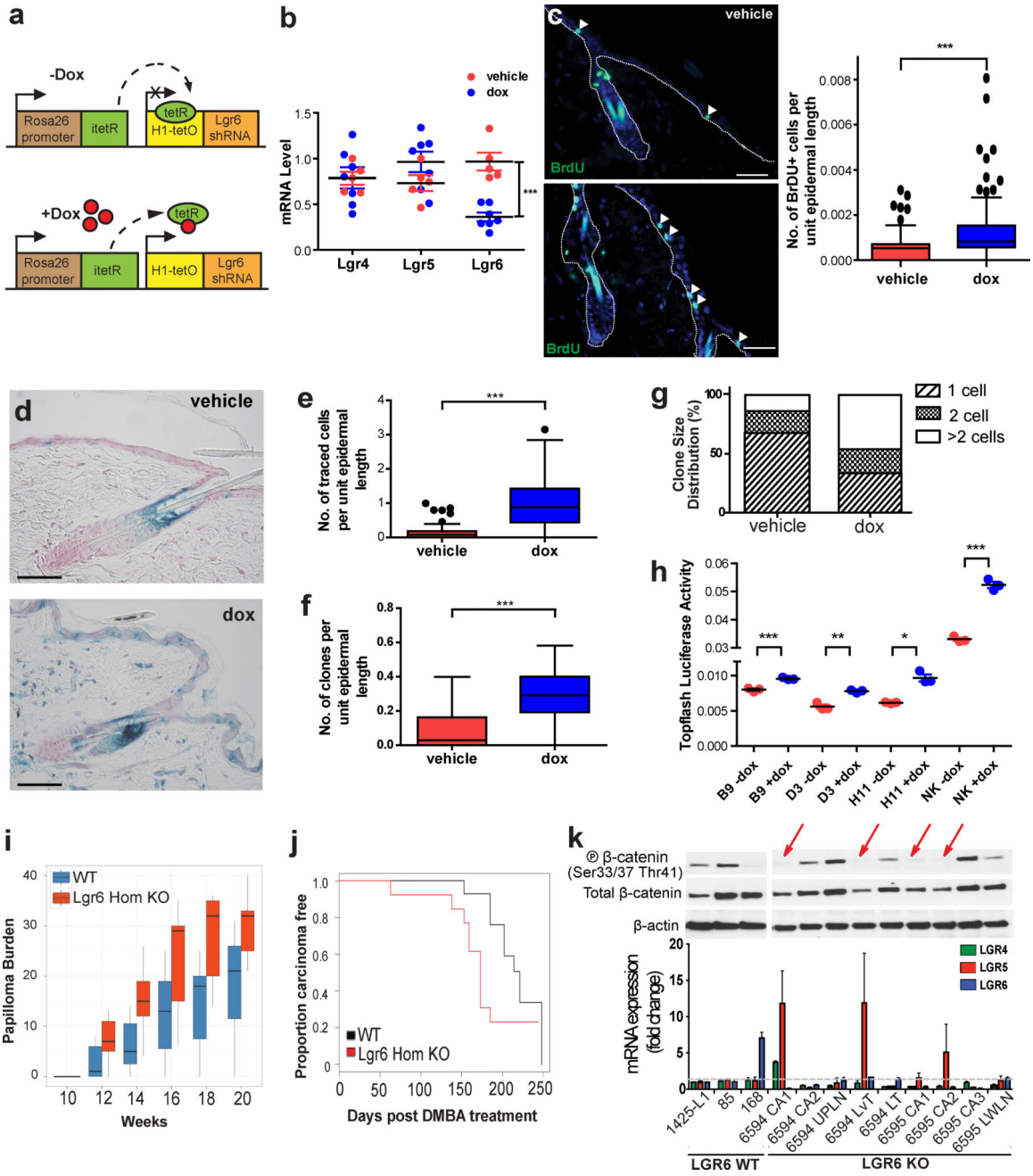

Figure 6. Lgr6 deficiency increases proliferation in the epidermis and leads to expanded Lgr6 lineage tracing into the epidermis

Adult *Lgr6 KD*$^{+/-}$ mice were administered doxycycline water or vehicle for 10 days. The animals were then intraperitoneally injected with BrdU and skin samples were harvested 3 h later. (**a**) Cartoon depicting mechanism of *Lgr6* knockdown induced by doxycycline treatment of *Lgr6 KD*$^{+/-}$ mice. In the absence of doxycycline, the tet repressor sits on the *H1-tetO* promoter[80] and prevents the transcription of the *Lgr6* shRNA. In the presence of doxycycline, the tet repressor is bound by the drug and prevented from associating with the *H1-tetO* promoter; this in turn allows for the transcription of the *Lgr6* shRNA. (**b**) *Lgr4-6*

mRNA levels in back skin samples were determined through Taqman analysis. (**c**) Top, example sections showing anti-BrdU immunofluorescence staining in back skin of *Lgr6 KD*$^{+/-}$ mice administered either vehicle (left) or doxycycline water (right). White arrowheads point to BrdU^{+} cells. Quantitation of anti-BrdU staining in vehicle- or doxycycline-treated *Lgr6 KD*$^{+/-}$ mice was also performed with 20 different fields of skin sections examined for each mouse. n ≥ 5 mice in each treatment group for (**b**) and (**c**). (**d**) Adult *Lgr6 KD*$^{+/-}$*/Lgr6-EGFP-IRES-CreERT2*$^{+/-}$*/R26RLacZ*$^{+/-}$ mice were administered either doxycycline water or vehicle. 10 days later, lineage tracing was induced with a topical dose of 4OHT; 7 days thereafter, skin samples were harvested and stained with X-Gal. (**d**) Representative sections showing X-Gal staining of skins from vehicle-treated (left) or doxycycline-treated (right) mice, n = 3 mice in each treatment group. (**e-g**) 20 different fields of skin sections were examined for each mouse to determine the number of traced cells per unit epidermal length (**e**), the number of Lgr6 clones per unit epidermal length (**f**) and the clone size distribution (**g**). Values lying further than 1.5 times the interquartile range in the box-and-whisker plots are plotted as dots. (**h**) A panel of normal and transformed epidermal cell lines was first transduced with an Lgr6 expression construct. Then, Lgr6 expression in these cells was either induced or left unperturbed through administering doxycycline or vehicle, respectively. After 2 days, Wnt activity was assessed using the TOPFlash luciferase reporter assay. n = 3. Adult *Lgr6*$^{+/+}$ and *Lgr6*$^{-/-}$ mice were initiated with a single dose of DMBA, then biweekly treatments of TPA for 20 weeks. (**i**) Papilloma burden by *Lgr6* genotype. Box-and-whisker plot depicting papilloma burden at 2 week intervals from week 10 to week 20 during DMBA/TPA mediated carcinogenesis. Mice are grouped and coloured by *Lgr6* genotype. The *Lgr6*$^{+/+}$ group consisted of 19 mice, and the *Lgr6*$^{-/-}$ group of 13 mice. Values lying further than 1.5 times the interquartile range are plotted as dots. Genotype is significantly associated with papilloma burden across all timepoints ($p < 0.05$ by ANOVA). (**j**) Carcinoma-free survival by *Lgr6* genotype. Kaplan-Meier plot for carcinoma-free survival in *Lgr6* WT and KO mice ($p < 0.05$ by log-rank test). The *Lgr6*$^{+/+}$ group consisted of 15 mice, and the *Lgr6*$^{-/-}$ group of 13 mice. Both cohorts consisted of approximately equal numbers of male and female mice. **(k)** Reactivation of Lgr5 expression and Wnt signalling in SCCs from Lgr6 knockout mice. The left panel shows heterogeneous activation of the Wnt pathway (denoted by a low level of the Phospho β-catenin) in tumours from wild type mice. The SCC with the highest level of Lgr6 expression (168 cells) has the strongest activation of the Wnt pathway. There is no expression of Lgr5 in SCCs from wild type mice. The right panel shows a series of 9 cell lines derived from Lgr6 knockout mice, of which 5 have strong activation of Wnt signalling. Four of these (denoted by the red arrows) have both low levels of Phospho-β-catenin and high levels of Lgr5.